FATIGUE LIMIT DETERMINATION BASED ON THE YIELD STRESS AND RESIDUAL STRESSES IN THE METAL SURFACE LAYER

A.V.Prokopenko*

There is an optimum depth for the residual stress location, which ensures the maximum fatigue limit. The optimum residual stress diagram is obtained empirically.

However, the shape of the optimum residual stress diagram can be calculated based of the metals fatigue fracture model for high-cycle loading presented below, which takes into account the state of the surface layer. There are local volumes in this layer with a lower yield stress, where a fatigue crack initiates when the amplitude of the applied variable stress exceeds the local yield stress. The crack growth rate in the surface layer depends on the local plastic strain and stress intensity factor ranges at a certain depth. The crack initiated on the surface gets arrested in the deeper layers where the reversed deformation is absent and the stress intensity factor is below the threshold one ΔK_{th} for a large crack. Here the following assumptions are made: the stress-strain diagrams for all the layers of the material are close to an ideal elastoplastic one; cyclic loading does not cause changes in the stress-strain diagrams. For titanium alloys and high-strength steels the hysteresis loop is absent at the fatigue limit and the surface layer experimental characteristics do not change after cyclic loading in a low-amplitude region. The ΔK_{th} value for long cracks is most commonly independent of the yield stress σ_Y, in some cases it increases with a decrease in σ_Y, and it never decreases. The ΔK_{th} value is assumed to be constant in the surface layer where σ_Y decreases.

The depth of the nonpropagating fatigue crack and the fatigue limit of the VT9 alloy with residual stresses differring in magnitude and in the depth of location were calculated from the $\sigma_Y - H$ dependence determined by the indentation method (where H is the distance from the surface) and from $\Delta K_{th} - R$ (R is the stress ratio in a cycle) with the account taken of the model assumptions ($\sigma_{0.2}$ = 1050 MPa, σ_u = 1150 MPa, ε = 10 %, ψ = 30 %). In the Figure the BAB_1C line indicates the depth of the nonpropagating fatigue crack H corresponding to the fatigue limit if residu-

* Institute for Problems of Strength
Academy of Sciences of the Ukr.SSR, Kiev, USSR

al stress to the right of this line decreases. A corresponding value of the fatigue limit is described by the DA_1E line and is obtained when the latter intersects the horizontal line from the point of the residual stress diagram intersection with the BAB_1CB_2 line. In the CB_1A region of the BAB_1C line the fatigue limit is found by solving the system of equations $\sigma_Y = f(H)$, $\sigma_a = f(H, R, \Delta K_{th})$. In the AB region the fatigue limit is not determined by the properties of the surface layer, since the residual stresses are high and lay deeper than the anomalous region. The sum of the extreme stress in a cycle and the residual stress exceeds the macroscopic yield stress in the core of the specimen inducing the reverse plastic deformation and crack extension. The A_1E line represents the difference between the value of the macroscopic yield stress σ_Y and the magnitude of the residual stress on the AA_2 line. This line sets a limit on the depth of the nonpropagating fatigue crack in the case when fatigue limit is determined as the $\sigma_Y - \sigma_o$ difference, i.e. beyond the boundaries of the surface layer.

Lines 1...5 in the Figure represent the residual stress diagrams in a surface layer of VT9 Ti-alloy specimens after different surface treatment and the corresponding calculated fatigue limits (crosses on the DA_1E line). These values are in fair agreement with the experimental fatigue limits (dots) from the data of Tseitlin (1).

The evaluation of the plastic zone size r_Y ahead of the crack of length in excess of 0.012 mm at the fatigue limit revealed the r_Y to the crack length ratio to be not less than 0.16...0.2 for the material of such a high strength as the VT9 alloy which allows the LEFM criteria to be used in calculations.

A tendency for an increase in the depth of the nonpropagating cracks with σ_o is supported by microscopic studies of pre-fatigued specimens.

There is another important aspect associated with a surface treatment of the components. As is seen in the Figure the depth of a nonpropagating fatigue crack grows with an increase in the fatigue limit caused by residual compressive stresses (B_1AB line). Such crack does not extend deep into the core if residual stresses arrest it. Yet they relax in service at the elevated temperature. If a surface-treated component is loaded with cyclic stresses of considerable magnitude for a short time, nonpropagating surface fatigue cracks appear in it which, after residual stress relaxation,

extend deep into the component and cause its failure. The fatigue limit of the component decreases. Line F in the Figure represents the fatigue limit after the residual stress relaxation if before the relaxation the component was loaded at the level of the fatigue limit determined by the DA_1E line. The determined role of residual stresses in the fatigue limit reduction for components operating at elevated temperature can be a key for discovering the reasons for fatigue fracture of components.

REFERENCE

(1) Tseitlin, V.I., Metallovedenie i termicheskaya obrabotka metallov (in Russian), No.4, 1979, pp.13-16.

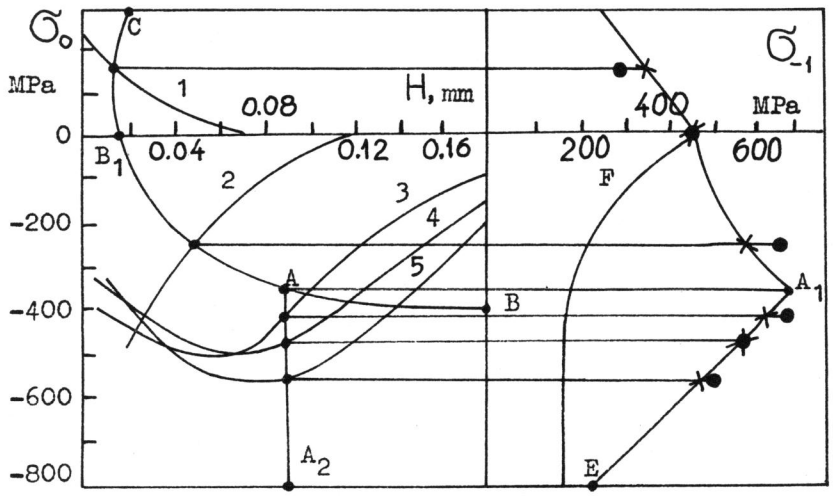

Figure Residual stress diagrams σ_0 (1...5), nonpropagating fatigue crack depth H and fatigue limit for the VT9 alloy specimens: (1) turning; (2) hardening by microballs; (3) pneumatic shot-blasting and vibropolishing; (4,5) hydro-shot blasting (experimental data from ref.(1)).